JOURNAL OF MATERIALS SCIENCE 30 (1995) 5328–5334

The yield behaviour of poly(phenylene-bibenzimidazole)

J. ROSE, R. A. DUCKETT, I. M. WARD
IRC in Polymer Science and Technology, University of Leeds, Leeds, LS2 9JT, UK

The compressive yield behaviour of poly(2,2′-m-phenylene-5,5′-bibenzimidazole) (PBI) has been studied over a wide range of temperatures. The tensile behaviour was also studied under superimposed hydrostatic pressure. In both cases wet and dry samples were examined and the results revealed the considerable effects of moisture on the mechanical properties of PBI. The results of all these tests show that PBI has a remarkably high shear yield stress at room temperature. This results in a very high compressive yield stress and a very high tensile yield stress observed under superimposed hydrostatic pressure when brittle failure from surface flaws is prevented. It is concluded on the basis of quantitative analysis that the yield mechanism in PBI at room temperature is initiation controlled, as in a metal or ceramic, rather than a velocity controlled, thermally activated, viscoelastic process which is generally considered applicable in polymers.

1. Introduction

Polybenzimidazoles are a class of polymers of high thermal stability and chemical resistance [1,2]. The mechanical behaviour of poly [2,2′-m-phenylene-5,5′-bibenzimidazole], commonly referred to by the acronym PBI, has been studied. The major issue considered was the remarkably high room-temperature compressive yield stress, which at 400 MPa, is much higher than most polymers, and raises the possibility of using PBI as the matrix in high-performance composites reinforced with carbon fibres. This very high compressive strength raises questions regarding its interpretation in terms of the mechanisms of yield. In this paper this topic will be explored, paying particular attention to the possibility that this is more akin to yielding in a glass and hence nucleation controlled, rather than relating to viscoelastic relaxation processes and hence velocity controlled. The latter is the more common situation in polymers at room temperature, which is generally comparatively close to the polymer melting point.

2. Experimental procedure

2.1 Materials

The PBI material for this project was provided by the Hoechst–Celanese Research Centre, Summit, NJ, in the form of 4 in × 4 in × 1/4 in (~10 cm × 10 cm × 0.65 cm) sheets formed by compression moulding in a matched-metal die using a vacuum hydraulic press. A few comparative tests were made on samples machined from a sintered rod of Vespel (e.g. [3]) (a polyimide from Du Pont) and on Perspex sheet (a high molecular weight PMMA, from ICI plc).

2.2 Compressive yield measurements

In accordance with the ASTM standard for compression tests on rigid plastics [4], rectangular blocks of size 6.35 mm × 6.35 mm × 12.7 mm (aspect ratio 2 : 1) were machined from the 1/4 in (~0.65 cm) sheets using the full thickness of the sheet as the long dimension. For comparison purposes samples of identical dimensions were tested of Vespel and PMMA.

The compression tests were carried out using a compression cage in an RDP-Howden servo mechanical testing machine. The load–extension curve was recorded on a chart recorder, and a correction applied for the machine compliance. The compressive yield point was taken as the maximum on the stress–strain curve, and the true strain, ε_t, at yield calculated as $\varepsilon_t = \log_e(h_0/h)$ where h is the corrected sample height at the yield point. Making the usual assumptions that there is no change of volume on deformation, the true yield stress, σ_t, is then calculated as $\sigma_t = F/A_0(1+\varepsilon_t)$, where F is the maximum load and A_0 the initial cross-sectional area.

It was found to be useful in each case to construct from the basic stress–strain curves subsidiary plots showing the secant compliance (strain/stress) plotted versus the applied strain.

The compressive yield behaviour was measured over the temperature range from $-90\,^{\circ}\mathrm{C}$ to $+150\,^{\circ}\mathrm{C}$ at strain rates of 10^{-2}, 10^{-3} and $3.3\times10^{-4}\,\mathrm{s}^{-1}$. Tests were carried out on both "wet" and "dry" PBI. Materials described as "dry" relate to compression specimens that had been placed in a vacuum oven at 180 °C for 24 h, and measured within a few hours of removal from the oven. "Wet" specimens had been placed in a bath of boiling water until the equilibrium water content (15% by weight) had been reached.

0022–2461

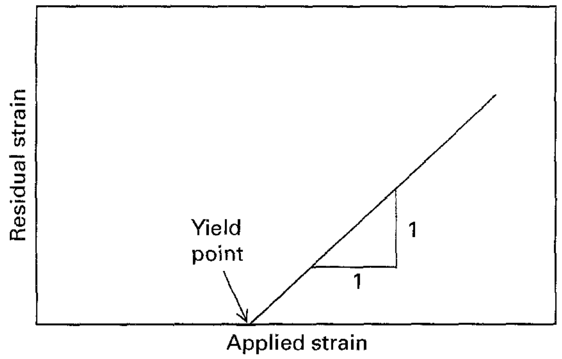

Figure 1 Ideal residual strain plotted against applied strain, showing yield as the onset of residual strain.

A second type of measurement was also undertaken. This was the determination of residual strain which is measured by unloading the sample subsequent to the application of a known strain. If this procedure is carried out for a range of applied strain values then a graph of residual strain against applied strain can be constructed. For an ideal elastic–plastic material the residual strain will be zero up to the yield point, and thereafter equal to the difference between the applied strain and the yield strain, as shown in Fig. 1.

2.3. High-pressure tests

Preliminary tensile tests at atmospheric pressure revealed that PBI is brittle, failing from surface irregularities at small strains. Tensile tests were therefore undertaken under a superimposed hydrostatic pressure because it is well established [5] that even brittle rocks can be induced to yield under sufficiently high pressures. As full details of the equipment and test procedure have been published previously [6], only a brief description will be given here. The test specimen was contained in a cylindrical steel pressure vessel. Pressure to the vessel was supplied by the hydraulic fluid (equal parts of castor oil and brake fluid) from a pressure intensifier. The pressure was measured by a strain gauge transducer, the output of which was also used to control the pressure via the action of a solenoid valve operating on the input to the intensifier. To avoid possible environmental stress cracking in the sample as a result of contact with the pressure fluid, the samples were protected from the pressure fluid by the use of a thin rubber sheath.

Tension was applied to the specimen by a pull rod that emerges from the vessel through a rubber seal. The opposite end of the pull rod was enclosed in another (“equalizing”) vessel to balance the end load, and equal pressure was maintained in the two vessels via an axial hole in the pull rod. A crosshead attached to the pull rod between the two vessels was moved at constant speed by the drive unit and screw threads of a commercial testing machine. The tensile load on the sample was sensed by strain gauges on the rods connecting the crosshead to the testing machine. The load–extension response of the rods is known and the small friction in the rubber seals was measured, allowing the load on the sample to be calculated.

2.4 Dynamic modulus measurements

Dynamic modulus measurements on PBI and Vespel were carried out over a wide temperature range in a Rheometrics RSA II apparatus using a three-point bending geometry. The PBI and Vespel sample dimensions were 6.9 mm × 3 mm × 50 mm and 6 mm × 4 mm × 50 mm, respectively. They were left at each temperature for 15 min and tested at an angular frequency of 10 rad s^{-1}.

3. Results

Typical compressive stress–strain curves for “wet” and “dry” samples of PBI tested at room temperature are shown in Fig. 2a. Fig. 2b summarizes the temperature dependence of the compressive yield stress data for different strain rates for both “wet” and “dry” samples. Typical residual strain results are shown in Fig. 3, from which it can be seen that both “wet” and “dry” samples show classical elastic–plastic behaviour. No time-dependent recovery of the residual strain could be detected over a period of several weeks. It is interesting to compare the results shown in Fig. 3 with the data obtained for Vespel shown in Fig. 4. Although the stress–strain curve for Vespel shows a yield point at about 15% strain, the residual strain data indicate that this polymer shows a degree of residual

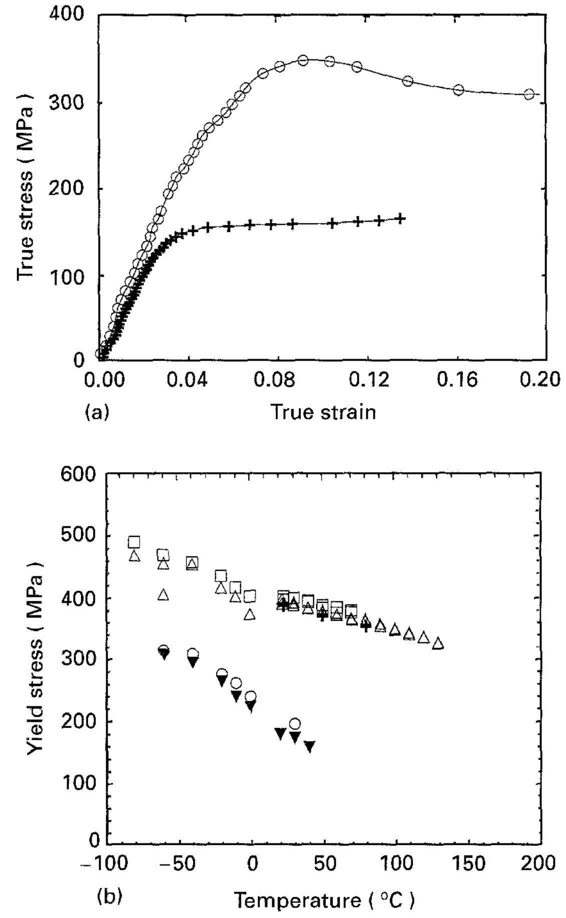

Figure 2(a) Comparison of the compressive stress–strain curves for (+) “wet” (15%) and (O) “dry” PBI at room temperature (strain rate 10^{-3} s^{-1}). (b) Compressive yield strength of (O, ▼) “wet” and (□, △, +) “dry” PBI as a function of temperature and strain rate: (□, O) 10^{-2}, (△, ▼) 10^{-3}, (+) 3.3×10^{-4}.

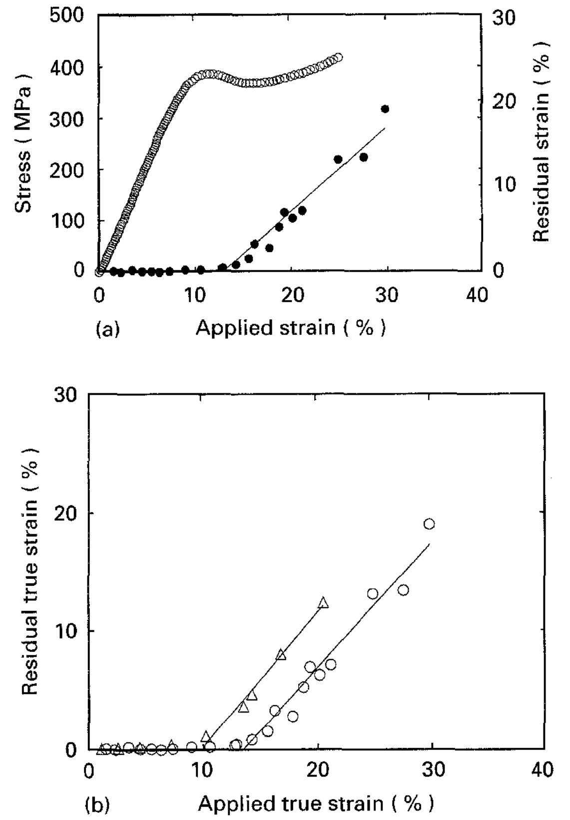

Figure 3(a) (O) Stress– strain curve for "dry" PBI at room temperature and $10^{-3}\,s^{-1}$ alongside results from the residual strain experiment. (b) Determination of the yield point of (△) "wet" and (O) "dry" PBI at room temperature and $10^{-3}\,s^{-1}$ by the residual strain method. (Note: both lines have been drawn with unit slope.)

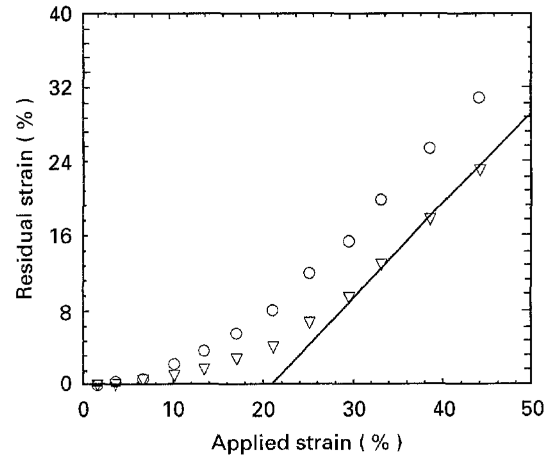

Figure 4 Determination of the yield point of Vespel by the residual strain method. (O) Immediate measurement of residual strain, (▽) residual strain measurement 2 weeks later. (Note: line has a slope of unity.)

strain even at very low strains, which is typical of viscoelastic behaviour.

A further interesting comparison was made with PMMA. Whereas at room temperature this polymer showed behaviour similar to Vespel, the compressive yield stress and residual strain characteristics at − 100 °C were very similar to PBI, as can be seen from Figs 5 and 6. A comparison of the results obtained for PBI and PMMA is shown in Table I.

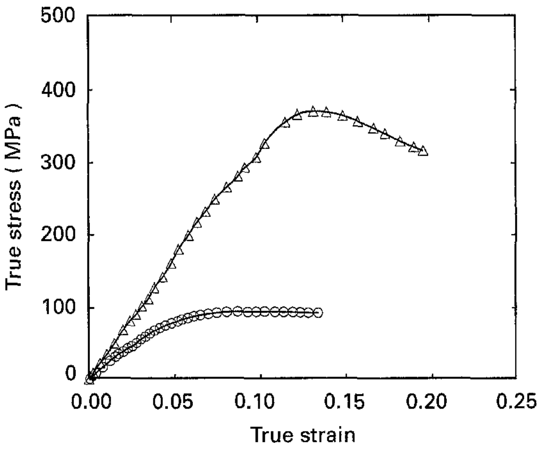

Figure 5 True stress–true strain curves for PMMA at (O) 25 and (△) − 100 °C ($10^{-3}\,s^{-1}$).

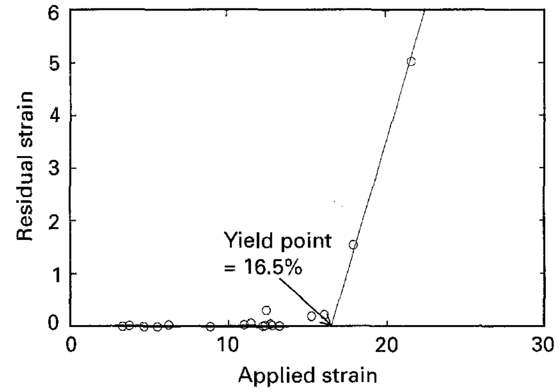

Figure 6 Determination of the yield point of PMMA at − 100 °C, $10^{-3}\,s^{-1}$ by the residual strain method. (Note: line has slope of unity.)

TABLE I Comparison of PBI and PMMA

	PBI	PMMA
Test temperature (K)	293	173
Glass transition, T_g(K)	698	378
T/T_g	0.429	0.457
Beta transition, T_β(K)	573	293
T/T_β	0.523	0.59
Compressive yield stress (MPa)	400	390
Strain to yield (%)	14.1	16.5

The key results from the high-pressure tensile tests are shown in Fig. 7. Results were obtained for the tensile stress–strain behaviour of both "wet" and "dry" PBI, tested under a hydrostatic pressure of 700 and 800 MPa, respectively. In the case of the test on "dry" material the tensile stress–strain curve has curved over and the maximum value of the stress obtained, 416 MPa, is just above that at which PBI yields in compression at atmospheric pressure. The tensile stress–strain curve at atmospheric pressure, on the other hand, is shown in Fig. 8. It can be seen that failure occurs at a stress of less than 100 MPa, and visual observation of the specimen confirmed that this was a brittle failure. From these results, taken together,

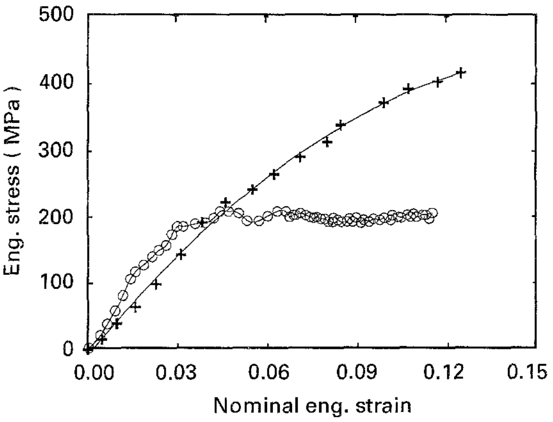

Figure 7 Tensile stress–strain curves for (○) "wet" (700 MPa) and (+) "dry" (800 MPa) PBI when tested under a hydrostatic pressure (room temperature, $10^{-3}\,s^{-1}$).

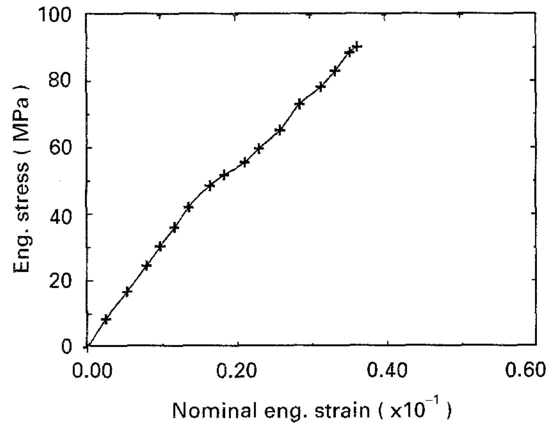

Figure 8 Tensile stress–strain curves for "dry" PBI at room temperature and (+) atmospheric pressure ($10^{-3}\,s^{-1}$).

it can be concluded that the tensile behaviour is normally dominated by flaws, and if the effect of these flaws is eliminated by the application of hydrostatic pressure, as discussed previously by Duckett [5], the behaviour in tension is also ductile.

Results are also presented in Fig. 7 for the "wet" material tested in tension under a superimposed hydrostatic pressure of 700 MPa. The polymer clearly yields before failure, and the value of the yield stress is 200 MPa, which is close to half the maximum value of 416 MPa found for the "dry" sample in these tests. These results are entirely consistent with the results shown in Fig. 2a for the compressive yield behaviour of "wet" and "dry" PBI.

It is clear that the unique feature of the mechanical behaviour of PBI is the very high value of the shear yield stress, which manifests as a very high compressive yield stress. It also results in a very high tensile yield stress in a situation, as in the case of superimposed hydrostatic pressure, where the failure in tension is not dominated by flaws. Otherwise brittle fracture occurs in tension at a comparatively low stress, before yield can occur. The residual strain results also point to a difference in kind between more conventional yielding in polymers, which relates more to non-linear viscoelastic behaviour, than to the classical elastic/plastic yield behaviour of metals and ceramics.

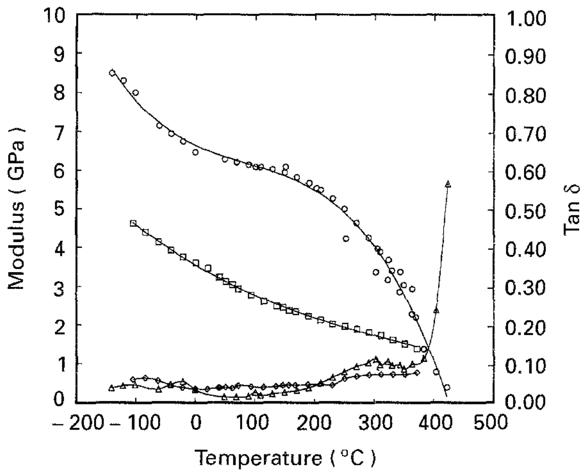

Figure 9 Bending modulus and tan data for PBI and Vespelas as functions of temperature (frequency 1 rad s^{-1}). PBI: modulus ○, tanδ △; Vespel: modulus □, tanδ ◇.

The results of the modulus measurements on PBI and Vespel are shown in Fig. 9.

4. Discussion

An important conclusion to be drawn from the results is that PBI at room temperature and PMMA at − 100 °C behave like elastic–plastic materials, and in both cases remarkably high values for the compressive, and hence the shear, yield stress are observed. It is proposed to develop the discussion along two lines. First, to consider the results for PBI in the context of current theories of yield behaviour for polymers. Secondly, to attempt to identify the structural features at a molecular level which could lead to the very high values of shear yield stress at room temperature.

4.1. Quantitative analysis of the yield behaviour

There are two principal approaches to discussing the yield behaviour of polymers, either to emphasize the thermally activated nature of the yield process using the Eyring formulation [7], in terms of an internal viscosity, or to consider that the yield process in a glassy polymer is analogous to that in a metal or ceramic, i.e. that it relates to the movement of dislocations or disclinations, as proposed by Bowden [8] and Argon [9] respectively.

The simpler approach, where yield is considered as a thermally activated process, can certainly describe the data for both "wet" and "dry" PBI very satisfactorily as shown in Fig. 10. The Eyring formulation gives

$$\dot{\gamma} = \dot{\gamma}_0 \exp -\left(\frac{\Delta H - \tau v}{kT}\right) \qquad (1)$$

where $\tau = \sigma/2$ is the shear yield stress at an applied strain rate $\dot{\gamma}$, ΔH and v are the activation energy and activation volume, respectively, $\dot{\gamma}_0$ the pre-exponential factor, T the absolute temperature, and k the Boltzmann constant.

This formulation applied to the PBI results gives activation volumes of 145 and 65.4 nm^3 for "dry" and "wet" polymer, respectively, as measured from

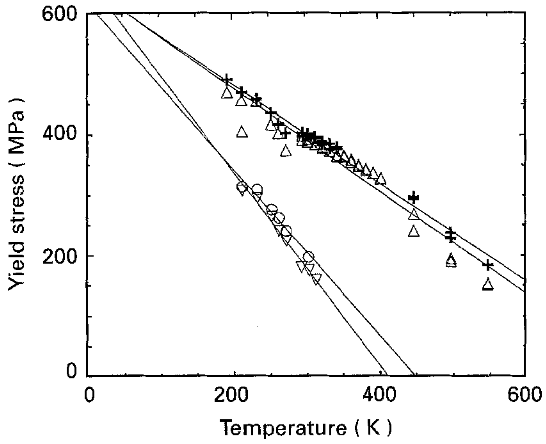

Figure 10 Eyring fit for the compressive yield of (○, ▽) "wet" and (+ , △) "dry" PBI as a function of temperature at strain rates of: (○, +) 10^{-2}, and (▽, △) $10^{-3}\,s^{-1}$.

$2v = kT/(d\sigma/d\log_e\dot{\varepsilon})_T$. These values are considerably smaller than those obtained by the same formulation for other isotropic polymers, e.g. polyethylene 6.5 nm^3 [10], polycarbonate (PC) 5.0 nm^3 [11], but is close to the volume of a monomer unit of PBI. When the clear evidence for elastic–plastic behaviour rather than viscoelastic behaviour is taken into account, it therefore appears more appropriate to explore an alternative approach, and for this the theory of Argon [9] has been chosen.

The Argon theory gives the shear yield stress, τ, as

$$\tau = \frac{0.102G}{(1-\nu)}\left[1 - \frac{16(1-\nu)kT}{3\pi G\omega^2 a^3}\log_e\left(\frac{\dot{\gamma}_0}{\dot{\gamma}}\right)\right]^{6/5} \quad (2)$$

where G, ν are the shear modulus and Poisson's ratio, respectively, a is the molecular radius, and ω is the angle of rotation in the molecular kink.

To compute a fit to the experimental data, the procedure proposed by Argon and Bessonov [12] was followed i.e. a graph of $(\tau/G)^{5/6}$ versus T/G was plotted using values for the shear modulus, G, calculated from the data in Fig. 9, assuming a Poisson's ratio of 0.3. The results shown in Fig. 11 confirm that this plot is a reasonable straight line and that the PBI data are broadly similar to those of other polymers considered by Argon and Bessonov.

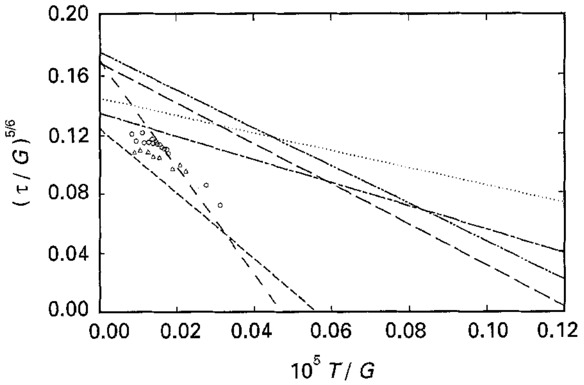

Figure 11 Argon model for PBI. (△) "wet" PBI, (○) "dry" PBI, (---) PPO (polyphenylene oxide), (···) Kapton (film-cast Vespel) (– – –) DFO (oxyaromatic polyimide [12]), (— - - —) PC, (— —) PMMA, (—— —) PET.

TABLE II Slopes and intercepts for Argon fit

Material	Intercept	Slope (MPaK^{-1})	ω^2a^3 (nm^3)
Kapton	0.145	0.060	1.65
DFO	0.135	0.080	1.24
PPO	0.125	0.223	0.444
PC	0.176	0.129	0.768
PET	0.169	0.138	0.718
PS	0.180	0.480	0.206
PMMA	0.170	0.364	0.272
PBI (dry)	0.142	0.203	0.419
PBI (wet)	0.130	0.198	0.392

As pointed out elsewhere previously ([7] p. 389), if the factor 6/5 in Equation 2 is replaced by unity, which makes a comparatively small numerical difference, this equation reduces to

$$\tau = \frac{0.102G}{1-\nu} - \frac{16\times 0.102kT}{3\pi\omega^2a^3}\log_e\frac{\dot{\gamma}_0}{\dot{\gamma}} \quad (4)$$

which is of similar form to the Eyring Equation 1 which can be written as

$$\tau = \frac{\Delta H}{v} - \frac{kT}{v}\log_e\frac{\dot{\gamma}_0}{\dot{\gamma}} \quad (5)$$

Equations 2 and 5 are almost indistinguishable in purely curve-fitting terms, except when data are available over an exceptionally wide range of temperatures and strain-rates. However it is very appealing that the collected data for PBI and a wide range of polymers whose yield behaviour was previously determined by Argon and Bessenov, do give intercepts on the $(\tau/G)^{5/6}$ versus T/G plots which are fairly close to $[0.102/(1-v)]^{5/6}$ (Table II). The parameter ω^2a^3 can also be calculated, assuming the "universal" value for $\dot{\gamma}_0$ of $3\times10^{13}\,s^{-1}$, and this relates directly, in the Argon theory, to the shear activation volume which is $5.3\,\omega^2a^3$. The collected values of ω^2a^3 in Table II, for all these polymers, including PBI, are generally in the range of 1 ± 0.5 nm^3. These values are, in general, more comparable with the monomer volumes than the higher values for activation volume obtained for polyethylene and polycarbonate using the Eyring formulation.

4.2. Molecular aspects of the yield behaviour

Having considered the analysis of the yield data in terms of current approaches to quantifying the yield behaviour of polymers, it is appropriate to address whether the apparent uniqueness of PBI in terms of its high shear-yield stress at room temperature can be understood in terms of other physical properties and ultimately the structure of the polymer.

In the first instance it is interesting to consider the proposal by Northolt [13] that the compressive strength of a polymer can be related to its glass transition temperature, T_g. This connection is based on the idea that compressive strength is governed by chain flexibility, which affects the glass transition temperature of the polymer. In Fig. 12, data from Van Krevelen [14] for the room-temperature compressive strength and T_g are plotted, together with the present

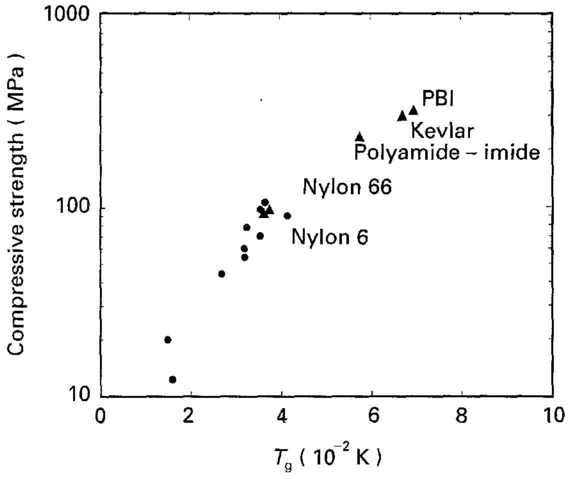

Figure 12 Compressive strength against glass transition, T_g, plot for a range of polymers.

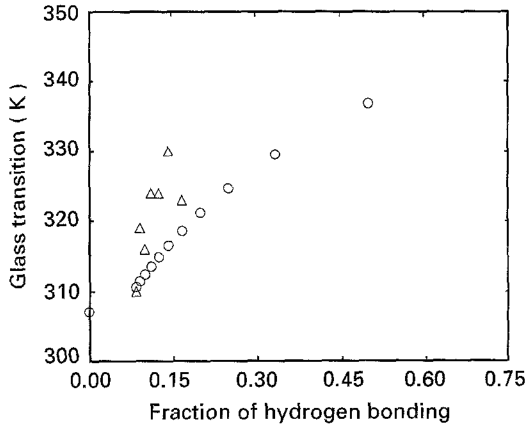

Figure 13 Effect of hydrogen bonding on the glass transition temperature of nylons: (○) calculated, (△) experimental.

result for PBI. It is clear that the empirical correlation proposed by Northolt holds quite well.

The glass transition of a polymer has been related to its structure by Van Krevelen on the basis of an empirical formula [14]

$$T_g = \frac{\sum_i Y_{gi}}{\sum_i M_i} \qquad (6)$$

where the contributions Y_{gi}, called the molar glass transition functions, are summed for i groups of the molar mass M.

Using data presented by Van Krevelen, Equation 6 predicts a T_g of 344 °C for PBI, which is significantly lower than the experimental value of 420 °C determined by DSC at a heating rate of 20 °C min^{-1}. This discrepancy could be due, in part, to the presence of hydrogen bonding in PBI between > N–H and N- groups on the imidazole groups of neighbouring chains, which has not been explicitly taken into account. For illustration of this possibility, Fig. 13 shows T_g for a range of nylons as a function of percentage of hydrogen bonding in the polymer, determined as the ratio of N–H groups to -CH_2- groups per repeat unit, with polyethylene taken as zero. The calculated values of T_g were obtained using Equation 6 with Van Krevelen's values for Y_g. It can be seen that T_g increases significantly with increasing proportion of hydrogen bonding.

A key observation from the experimental data on PBI is the major difference between the yield stresses for "dry" and "wet" PBI. It seems likely that this arises due to reduction in intermolecular forces when the polymer is swollen with water and the linear dimensions increase by 4%. Assuming uniform swelling this corresponds to an increase in chain spacing of $\sim$4%, which has been confirmed by broad-line nuclear measurements magnetic resonance [15]. The strength of Van der Waals forces is inversely proportional to the interchain spacing raised to the power six. This increase in chain spacing would therefore lead to a reduction in the Van der Waals forces of approximately 20%. The actual reduction in shear stress is about 50%, suggesting that there is a reduction of intermolecular forces due to the reduction in hydrogen bonding forces as well as the Van der Waals dispersion forces.

Finally, it is of interest to consider the observation that PBI behaves as an ideal elastic–plastic material at room temperature, and this is also true for PMMA at − 100 °C. In general intuitive terms, it appears that at temperatures well below T_g, there is no way that stress can cause changes in the conformational states by biasing thermally activated processes, as envisaged by the theories based on Eyring-type site model theories, i.e. the activation energy for a transition is much greater than the thermal energy, kT. It may also be that secondary transitions (β-transitions) have some importance in this respect.

In PBI there are two groups in the structure that are able to rotate, the *m*-phenylene ring and the benzimidazole rings. Goswell and Levine [16] suggest that the β relaxation in PBI is due to the rotation of the *m*-phenylene ring and that T_g is due to the rotation of the benzimidazole ring structure. Below T_β there is therefore no rotation of any group within the structure.

Fig. 14 shows a model of the PBI repeat unit, constructed using the BIOSYM molecular modelling software, which indicates that the phenylene ring in the PBI unit does not lie in line or in plane with the rest of the structure. Therefore, in the solid polymer we have a rigid chain which contains many "kinks" along its length. The only way for such a chain to slide past another chain when all molecular rotations are quenched is to create a hole by elastic distortion of bond angles, big enough to allow chains to slide past each other. This would require large amounts of energy and is consistent with the material having a high yield strength. Also, after deformation there would be no recovery as the forces to create the necessary free volume would be much greater than entropic recovery forces.

For PMMA we have a similar situation. The glass transition is associated with the rotation about C–C bonds in the main chain and the β relaxation is thought to be due to the mobility of the side groups. Below T_β there is no mobility in the system. The configuration of syndiotatic PMMA has been shown by Lovell and Windle [17] to form a curved structure. Again, deformation of this structure would require elastic bending of the molecule to allow chains to move past each other.

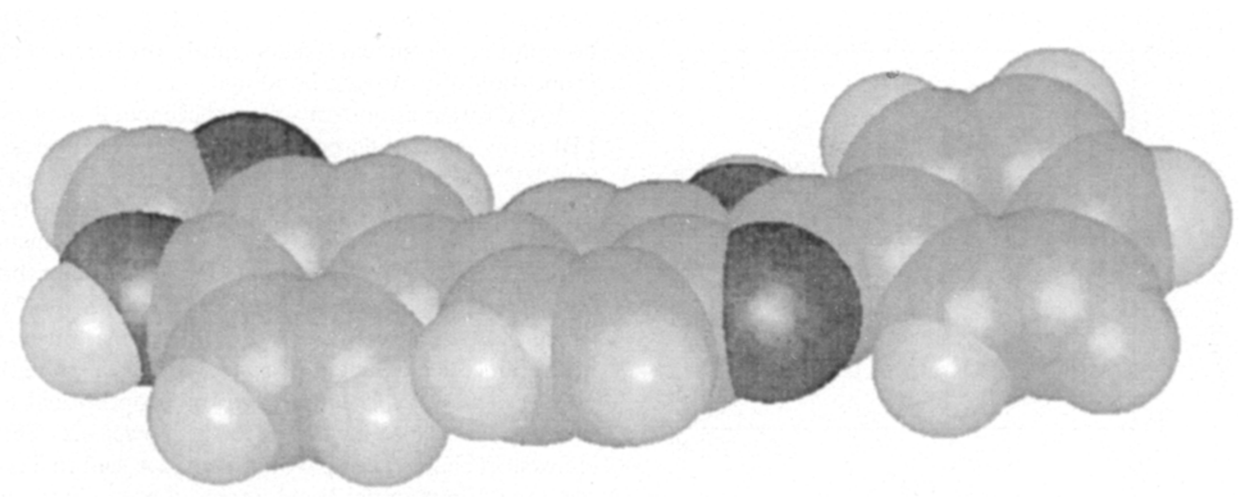

Figure 14 Model of the PBI repeat unit drawn using the BIOSYM molecular modelling system.

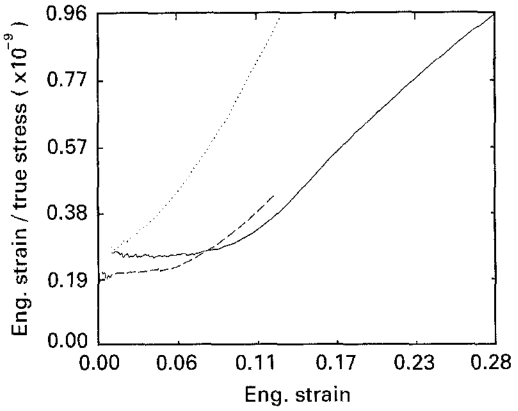

Figure 15 Compliance–strain plots for PBI at (—) 20, (- - -) 130 and (···) 275 °C, showing the initial linear region decreasing in extent as the temperature increases (strain rate $10^{-3}\,s^{-1}$).

In both cases the elastic bending of the structure would result in an approximately linear stress–strain response. If the energy required to deform the structure is the sum of the thermal energy and the supplied mechanical energy, then as the temperature is increased the amount of mechanical energy that needs to be supplied, will decrease. As a result the strains at which the linear elastic response is observed should decrease as the test temperature is increased.

Further insight into the differences in behaviour above and below the β-transition is afforded by the plots of compliance versus strain shown in Fig. 15. Under low-temperature conditions for which the residual strain plots show conventional elastic–plastic behaviour, the compliance is, of course, independent of strain at low strains. At higher temperatures the behaviour can be more accurately described as non-linear viscoelastic, because the compliance is strain-dependent from extremely low strains, and the "residual" strain exhibits some time-dependent recovery.

5. Conclusion

The compressive yield stress results for PBI have been considered in the light of current theories of the yield behaviour of polymers. It is concluded that it is most appropriate to consider that the yield mechanism is more akin to that occurring in a crystalline solid such as a metal or a ceramic, than that normally occurring in polymers where viscoelastic deformation occurs primarily due to molecular flow as in a viscous liquid.

At a molecular level it is proposed that the high yield stress and high modulus of PBI at room temperature are linked to the very high glass transition temperature of the polymer, due to the very stiff polymer chain backbone which also has some capability of hydrogen bonding. The fact that the behaviour below the yield point is so clearly linear elastic is attributed to the kinked molecular chain which does not permit easy shear at temperatures below the β relaxation where there is no molecular mobility. It is significant that PMMA displays similar behaviour when tested at an equivalent temperature below its β relaxation.

References

1. E. J. POWERS and G. A. SERAD, in "High Performance Polymers: Their Origin and Development", edited by R. B. Seymour and G. S. Kirshenbaum (Elsevier Applied Science, New York, 1986) p. 355.
2. A. BUCKLEY, D. E. STUETZ and G. A. SERAD, in "Encyclopedia of Polymer Science and Engineering" Vol. 11 (Wiley, New York, 1988) p. 572.
3. J. A. BRYDSON, "Plastics Materials", 5th Edn (Butterworths, 1989) p. 4867.
4. ASTM D 695 M - 85 (American Society for Testing and Materials, Philadelphia, PA, 1985).
5. R. A. DUCKETT, *J. Mater. Sci.* **15** (1980) 2471.
6. J. SWEENEY, R. A. DUCKETT and I. M. WARD, *Proc. R. Soc. Lond.* **A420** (1988) 53.
7. I. M. WARD, "Mechanical Properties of Solid Polymers", 2nd Edn, (Wiley, Chichester, 1983) p. 377.
8. P. B. BOWDEN and S. RAHA, *Philos. Mag.* **29** (1974) 149.
9. A. S. ARGON, *ibid.* **28** (1973) 839.
10. R. W. TRUSS, P. D. CLARKE, R. A. DUCKETT and I. M. WARD, *J. Polym. Sci. Polym. Phys. Edn* **22** (1984) 191.
11. C. BAUWENS-CROWET, J. A. BAUWENS and G. HOMÈS, *J. Polym. Sci.* **A2**(7) (1969) 735.
12. A. S. ARGON and M. I. BESSONOV, *Philos. Mag.* **35** (1977) 917.
13. M. G. NORTHOLT, *J. Mater. Sci.* **16** (1981) 2025.
14. D. W. VAN KREVELEN, "Properties of Polymers", 3rd Edn (Elsevier Applied Science, Amsterdam, 1990) p.129 ff.
15. N. W. BROOKS, R. A. DUCKETT, J. ROSE and I. M. WARD, *Polymer* **34** (1993) 4038.
16. R. B. GOSWELL and H. H. LEVINE, *J. Macro. Sci. Chem.* **A3** (1969) 1381.
17. R. LOVELL and A. H. WINDLE, *Polymer* **22** (1982) 175.

Received 9 May
and accepted 7 June 1995